Soils and Foundations 2014;54(1):67–80

The Japanese Geotechnical Society

Soils and Foundations

www.sciencedirect.com
journal homepage: www.elsevier.com/locate/sandf

Medium-size triaxial apparatus for unsaturated granular subbase course materials

Tatsuya Ishikawa[a,*], Yuan Zhang[b], Tetsuya Tokoro[c], Seiichi Miura[d]

[a]*Laboratory of Analytical Geomechanics, Faculty of Engineering, Hokkaido University, Kita 13, Nishi 8, Kita-ku, Sapporo 060-8628, Japan*
[b]*Graduate School of Engineering, Hokkaido University, Japan*
[c]*Tomakomai National College of Technology, Japan*
[d]*Faculty of Engineering, Hokkaido University, Japan*

Received 30 November 2012; received in revised form 24 May 2013; accepted 17 June 2013
Available online 24 January 2014

Abstract

This paper proposes a testing method for evaluating the effect of water content on the deformation–strength characteristics of unsaturated subbase course materials. A medium-size triaxial apparatus for unsaturated soils is newly developed in order to examine the mechanical behavior of unsaturated subbase course materials subjected to fluctuations in water content and to shorten the testing time. It adopts the pressure membrane method with hydrophilic microporous membrane filters, instead of the pressure plate method with ceramic disks, and controls both pore air pressure and pore water pressure at the cap and the pedestal separately. The results of the proposed testing method, carried out by this apparatus, are shown to conform well to the results of previous researches. This indicates that the medium-size triaxial apparatus for unsaturated soils is highly useful for triaxial compression tests and water retentivity tests on unsaturated granular base course materials and for shortening the total testing time.

Keywords: Base course; Cyclic load; Pavement; Triaxial test; Water retentivity test; Unsaturated soil; Water content; IGC: D06; E10; H06

1. Introduction

In cold snowy regions, such as Hokkaido, the 0 °C isotherm may penetrate deep into pavements, thereby causing the upheaval of pavement surfaces or the cracking of the asphalt-mixture layer arising mainly from the frost heave of the subgrade. Furthermore, the water content rises in the unsaturated subbase course and the subgrade owing to the infiltration of thaw water and the thawing of ice lenses during the thawing season, resulting in the temporary degradation of the bearing capacity and the stiffness (Ishikawa et al., 2012). Such phenomena specific to cold regions are thought to accelerate the deterioration of pavement structures and the loss of functions. In turn, freeze–thawing greatly affects the decrease in the fatigue life of pavement structures. For example, the mechanistic-empirical pavement design guide (MEPDG; AASHTO, 2008) can evaluate the effects of environmental factors, such as water content, on the fatigue life by using the model proposed by Cary and Zapata (2010). Therefore, to rationalize a design method for transportation infrastructures better suited to the climatic conditions of cold snowy regions, it is of great significance to improve the theoretical design method adopted in Japan (Japan Road Association, 2006), so that it can be applied to evaluate the

*Corresponding author. Tel./fax: +81 11 706 6202.
E-mail address: t-ishika@eng.hokudai.ac.jp (T. Ishikawa).
Peer review under responsibility of The Japanese Geotechnical Society.

Production and hosting by Elsevier

0038-0806 © 2014 The Japanese Geotechnical Society. Production and hosting by Elsevier B.V. All rights reserved.
http://dx.doi.org/10.1016/j.sandf.2013.12.007

changes in the hydro-mechanical characteristics of unsaturated base course and subgrade materials caused by freeze–thawing. Based on these circumstances, we focus our research on the mechanical behavior of unsaturated granular subbase course materials, which suffer from the seasonal fluctuations in water content due to freeze–thaw as well as rainfall infiltration and variations in groundwater level, in order to propose a mathematical model for predicting the mechanical response of unsaturated subbase course during the thawing season and to incorporate the model into the theoretical design method for asphalt pavements.

The "Method of Test for Modified California Bearing Ratio (E001)" and the "Method of Test for Resilient Modulus of Unbound Granular Base Material and Subgrade Soils (E016)" have been specified by the Japan Road Association (2007) as the testing methods for subbase course materials used in the design calculations of pavement structures. However, these testing methods were generally designed to examine the deformation–strength characteristics of subbase course materials with optimum water contents, and not to evaluate the effects of water content on the mechanical behavior in a detailed manner. Accordingly, the mechanical behavior of unsaturated base course materials has not yet been sufficiently clarified by laboratory element tests here in Japan.

Meanwhile, progress in unsaturated soil testing technology enables the control and the measurement of matric suction in a variety of laboratory element tests for unsaturated soils (Fredlund, 2006). As a laboratory element test on unsaturated base course materials, which have a maximum particle size over 20 mm, various testing methods have been proposed in accordance with the research objectives and the experimental conditions to evaluate the deformation–strength characteristics and the water retention–permeability characteristics (e.g., Kolisoja et al., 2002; Coronado et al., 2005; Ekblad and Isacsson, 2008; Zhang et al., 2009; Yano et al., 2011; Craciun and Lo, 2012). For example, as a water retentivity test for subbase course materials, which have a maximum particle size of almost 40 mm, Yano et al. (2011) employed the suction method (water-head type), while Ishigaki and Nemoto (2005) employed the soil column method. Moreover, Yano et al., 2011 conducted permeability tests on unsaturated subbase course materials using a steady-state method (flux-control type). However, the mechanical behavior of unsaturated subbase course materials has not yet been sufficiently clarified in Japan by laboratory element tests, although shear tests on unsaturated granular subbase course materials have been conducted overseas by measuring the matric suction. Those tests have revealed that the resilient modulus of unsaturated base course materials decreases with the increase in water content (Coronado et al., 2005; Ekblad and Isacsson, 2008). This is because laboratory element tests on unsaturated soils with large-size specimens are quite time-consuming due to the ceramic disk with very low permeability that is usually used in the test apparatus for unsaturated soils. For a detailed examination of the deformation–strength characteristics of unsaturated base course materials, therefore, it is indispensable that a new medium-size triaxial apparatus to be developed for these unsaturated soils, which can reduce the testing time as well as examine the deformation–strength characteristics of granular base course materials under various degrees of compaction and water contents with high precision under sufficiently controlled experimental conditions.

In this study, we newly propose a suction-controlled laboratory element test for the mechanical properties of granular subbase course materials that adopts unsaturated soil testing technology, such as the axis translation technique, in order to quantitatively evaluate the effects of increased water content inside the base course layer during the thawing season on the long-term performance of pavement structures.

2. Test apparatus

2.1. Development plan for test apparatus

Since unsaturated coarse-grained soils, such as subbase course materials, show low suction of 100 kPa or lower (Ekblad and Isacsson, 2008; Zhang et al., 2009), it is assumed that test methods capable of measuring in the low-suction range, such as the soil column method, the suction method, and the pressure method, are appropriate for this type of soil. In particular, the pressure method is suitable as a laboratory element test for evaluating the mechanical properties of unsaturated subbase course materials because it has a wider measuring range than either the soil column method or the suction method. While the pressure method can be classified into a pressure plate method that utilizes a ceramic disc, and a pressure membrane method that utilizes a microporous membrane filter, the former is more widely used. However, ceramic discs are extremely low in water permeability; and thus, the testing time would be extremely long in suction-controlled shear tests for specimens with large diameters, such as the tests for subbase course materials.

To solve this problem, Nishimura et al. (2012) and Ishikawa et al. (2010) recently conducted some laboratory element tests on unsaturated soils with the pressure membrane method, using a microporous membrane filter instead of a ceramic disc, and reported that the pressure membrane method was useful in shortening the testing time. Thus, we developed a medium-size triaxial apparatus for unsaturated soils, which adopts the pressure membrane method, to evaluate the deformation–strength characteristics of base course materials in an unsaturated condition. This study evaluates the applicability and the utility of a testing method using the newly developed medium-size triaxial apparatus to laboratory element tests for the mechanical properties of unsaturated subbase course materials in terms of the validity of the test results and a reduction in the total testing time. For this purpose, a series of water retentivity tests and triaxial compression tests on unsaturated sand and crusher-run was carried out.

2.2. Medium-size triaxial apparatus for unsaturated soils

A schematic diagram of the medium-size triaxial apparatus for unsaturated coarse granular materials is shown in Fig. 1.

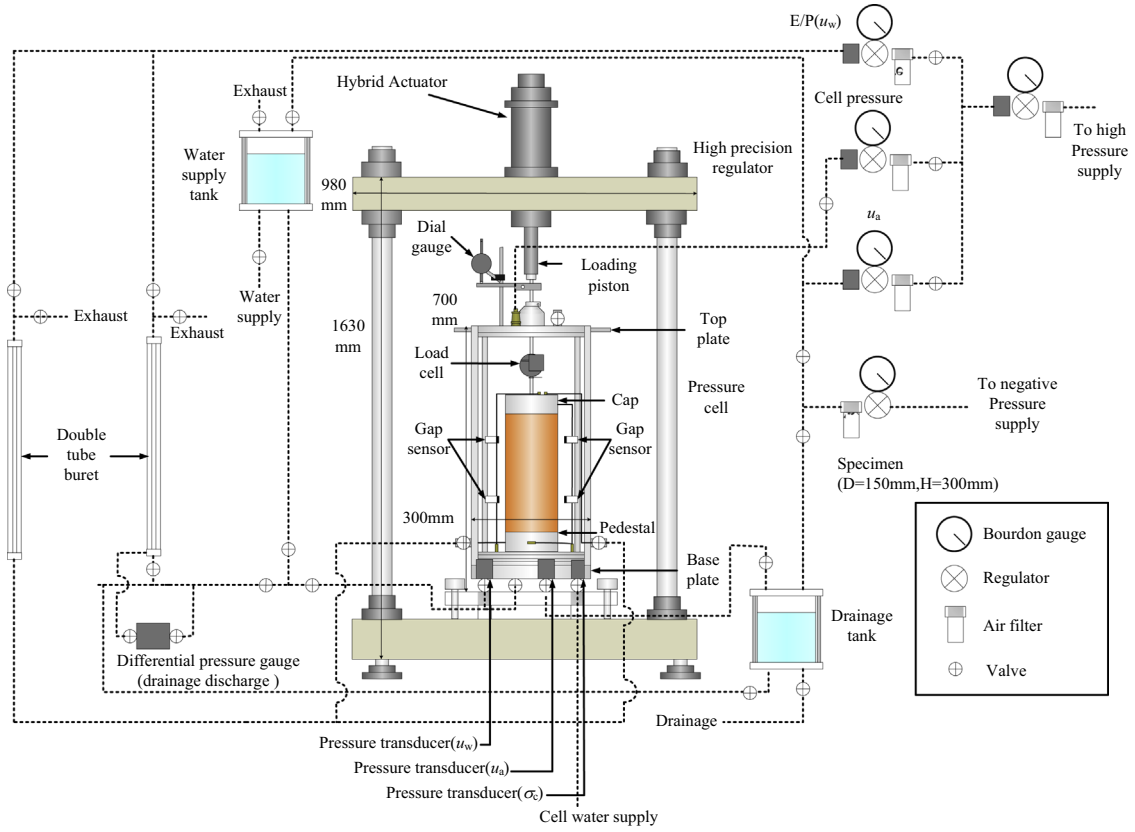

Fig. 1. Medium-size triaxial apparatus for unsaturated soils.

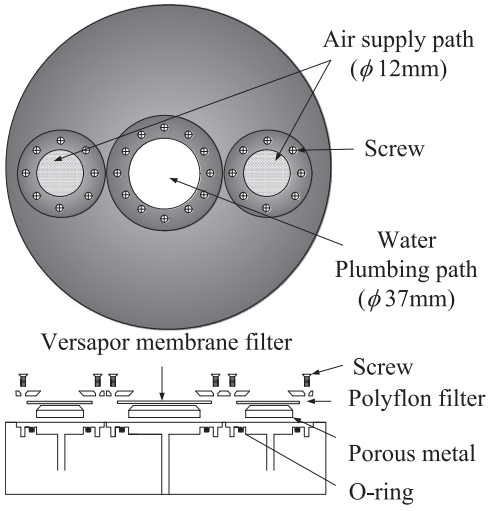

Fig. 2. Structure of cap and pedestal.

One key feature of the apparatus is the structural design of the cap and the pedestal, as shown in Fig. 2. Pore water pressure is applied to a specimen through a versapor membrane filter attached to the water plumbing path, while pore air pressure is applied through a hydrophobic polyflon filter attached to the air supply path in the cap and the pedestal. Here, the versapor membrane filter is a kind of microporous membrane filter made from a hydrophilic acryic copolymer. The physical properties of the filters are provided in Table 1. Other key features of the apparatus are as follows:

Table 1
Physical properties of filters.

Name	Thickness (μm)	Pore size (μm)	AEV/WEV (kPa)	k (m/s)
Versapor	94.0	0.8	60.0	4.4×10^{-8}
Polyflon	540.0	–	14.9	–

(1) Since the apparatus can handle a medium-size cylindrical specimen with an initial height (H) of 300 mm and a diameter (D) of 150 mm, triaxial compression tests can be implemented pursuant to the "Standard Method of Test for Determining the Resilient Modulus of Soils and Aggregate Materials (AASHTO Designation: T307-99)" (AASTHO, 2003) or the "Method of Test for Resilient Modulus of Unbound Granular Base Material and Subgrade Soils (E016)" (Japan Road Association, 2007).

(2) A pore water pressure path and a pore air pressure path are connected to the cap and the pedestal, respectively, which enables the control of matric suction and the supply/drainage of pore water from both ends of the specimen (Fig. 2). In addition, a flushing path is also installed on both the cap and the pedestal so that the water supply/drainage paths can be saturated easily.

(3) The apparatus can apply axial loads to a specimen with high precision by both the strain control method and the stress control method with only one hybrid actuator, which is equipped with a hydraulic servo control system adopting the feedback control method. Accordingly, the apparatus can perform both monotonic loading tests, at a very slow loading rate, and cyclic loading tests, in which the maximum frequency of the cyclic loading reaches about 10 Hz.

The measurements of stress and strain in a specimen were performed as follows. The axial stress (σ_a) was measured by a load cell installed inside the triaxial cell. The axial strain (ε_a) was obtained by measuring the axial displacement with two linear variable differential transformers (LVDTs), installed on the top of the cap inside the triaxial cell, and an external displacement transducer (dial gauge, EXT), installed on the upper plate (Fig. 3). Moreover, as bedding errors (Burland, 1989; Tatsuoka et al., 1995) seriously influence the deformation behavior of unbound granular base materials (e.g., Nazarian et al., 1997; Tutumluer et al., 1998; Dawson and Gillett, 1998), axial strain (ε_a) up to 2% was measured by two LVDTs (hereafter referred to as "LLVDT") attached at the center of the specimen, in parallel with two side lines located at the diagonal position pursuant to AASHTO T274-82 (AASHTO, 1986). Meanwhile, volumetric strain (ε_v) was mainly calculated based on the lateral displacements of the specimen, namely, the change in specimen diameter, measured by two sets of two proximity transducers (gap sensors, GSs) initially attached at the points of 1/4 and 3/4 of the specimen height diagonally opposite to each other around the specimen diameter, respectively. The calculation method of ε_v using GSs will be shown in the latter part of this paper. In the case of a saturated specimen, the volume of drainage during testing was also measured with a double tube buret.

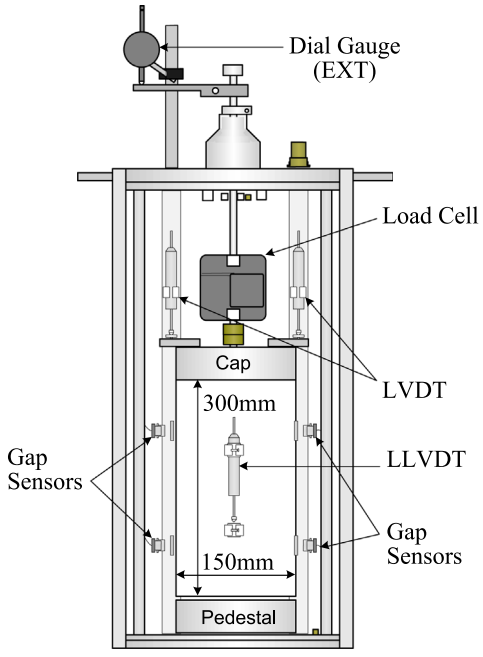

Fig. 3. Setting of displacement measurement devices.

3. Testing methods

3.1. Preparation of test specimens

Toyoura sand and a subbase course material, "C-40", are employed as the test materials. The physical properties and the grain-size distribution curves for the test samples are shown in Table 2 and Fig. 4, respectively. Toyoura sand is a type of Japanese standard sand, employed as a test material by many researchers in laboratory element tests, while C-40 is natural crusher-run made from angular, crushed, hard andesite stone used in Japanese roads as a base course material. Although the grading of the original C-40 material has a grain-size distribution of 0–40 mm, the C-40 material in this study is prepared by screening out particles larger than 37.5 mm from the original one pursuant to AASHTO T307-99 (AASTHO, 2003). Note that Toyoura sand did not show particle crushability at the low stress levels employed in this study, while a small amount of particle breakage due to compression and shear during triaxial compression tests could be discerned for C-40 according to the results of the sieve analysis before and after testing.

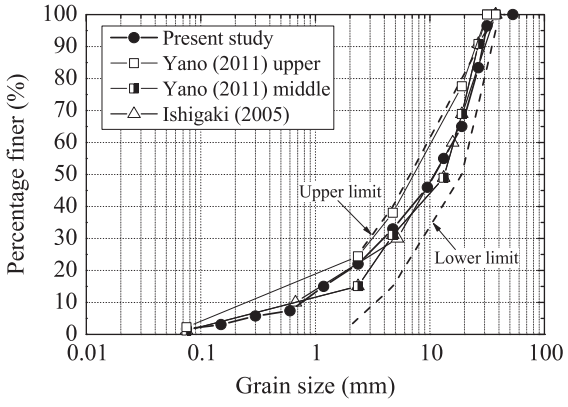

Fig. 4. Grain size distributions of C-40 materials.

Table 2
Physical properties of test materials.

Name	ρ_{dmax} (g/cm^3)	W_{opt} (%)	F_c (%)	PI	ρ_s (g/cm^3)	U_c	D_{50} (mm)	ρ_{dmax} (g/cm^3)	ρ_{dmin} (g/cm^3)
Toyoura	1.850	13.6	0.0	NP	2.65	1.3	0.18	1.648	1.354
C-40	2.070	8.2	1.7	NP	2.74	37.1	9.1	2.270	1.680
Yano (2011) middle	2.062	2.0	1.2	NP	–	23.9	–	–	–
Ishigaki (2005)	2.105	3.0	–	NP	2.65	23.6	–	–	–

Test specimens were prepared as follows. A cylindrical specimen for Toyoura sand was prepared with an oven-dried sample using the multiple-sieve pluviation method (MSP method, Miura and Toki, 1982). The initial dry density (ρ_{d0}) was adjusted so that the relative density (D_r) after consolidation would be 85% for uniform specimens with low variations in density. On the other hand, a cylindrical specimen for C-40 was prepared with an air-dried sample by tamping with a wooden rammer and compacting with a vibrator in five layers. The air-dried sample with a water content (w) of 1.2% was placed into a cylindrical mold in steps and spread into a layer with a thickness of 60 mm. Subsequently, each layer was compacted by a vibrator mounted on top of the sample for a certain period with constant compaction energy so as to attain the degree of compaction (D_c) of 95%. Note that fine particles with a grain size under 2 mm, which were collected from the top and bottom layers among the above-mentioned compacted five layers so as not to change the grain-size distribution, are spread on both ends of the specimen with a thickness of about 5 mm so as not to degrade the function of the filters installed on both the cap and the pedestal due to the direct contact with the coarse particles. In this study, we refer to this sample as the "air-dried specimen"; its degree of saturation (S_r) is 8.2%.

3.2. Water retentivity tests

Water retentivity tests on Toyoura sand and C-40 were carried out as per the "Test method for water retentivity of soils (JGS, 2009)" as follows. After preparing the air-dried specimen, it was permeated from the bottom end by de-aired water. Subsequently, the specimen was isotropically consolidated under a prescribed net normal stress (σ_{net}) of 49.0 kPa for 24 h by applying cell pressure (σ_c) of 249 kPa, pore air pressure (u_a) of 200 kPa, and pore water pressure (u_w) of 200 kPa. Here, σ_{net} is defined as $\sigma_{net}=\sigma_c-u_a$. After isotropic consolidation, a water retentivity test was initiated at a nearly saturated condition, and it proceeded through a drying process by decreasing u_w in steps, while keeping both σ_c and u_a constant, in other words, by applying a higher matric suction (s) to the specimen. Here, s is defined as $s=u_a-u_w$. An increase in s causes the drainage of pore water from the specimen. Upon attaining an equilibrium condition, the drainage was stopped and the water content corresponding to the applied matric suction was computed by reading the change in water volume during each increment in matric suction with a double tube buret. The above-described procedure was then repeated for higher values of matric suction until the desired range for the drying curve in a soil–water characteristic curve (SWCC) was obtained. Note that the volumetric change of the specimen could hardly be discerned during the water retentivity test.

3.3. Triaxial compression tests

Two types of triaxial compression tests were performed on the C-40 material, that is, monotonic loading tests and cyclic loading tests, under three different water contents, "air-dried", "unsaturated", and "saturated," in conformance with the standards of the Japanese Geotechnical Society (JGS, 2000a, 2000b) or the AASHTO T307-99. Note that the test data for the unsaturated condition was arranged by using the net normal stress (σ_{net}) instead of the effective confining pressure (σ'_c) under air-dried and saturated conditions.

3.3.1. Monotonic loading tests

The consolidated specimen of C-40 under saturated, unsaturated, or air-dried conditions was set up as follows. For the air-dried specimen ($S_r=8.2\%$), the specimen was isotropically consolidated after preparation under a prescribed effective confining pressure (σ'_c) of 49 kPa for 24 h by applying a designated negative pore air pressure (u_a) of -49 kPa. For the saturated specimen ($S_r=100\%$), carbon dioxide gas was added from the bottom end of the specimen after preparation for 30 min, and subsequently, permeating de-aired water into the voids for around 5 h. A back pressure of 200 kPa was then applied to ensure the saturation of the specimen and to achieve a pore water pressure coefficient B-value of 0.96 or higher. Following the saturation, the specimen was isotropically consolidated under a specified effective confining pressure (σ'_c) of 49.0 kPa for 24 h by applying a designated cell pressure (σ_c) of 249 kPa and pore water pressure (u_w) of 200 kPa. For the unsaturated specimen ($S_r=36.7\%$), a specimen under a prescribed net normal stress (σ_{net}) of 49.0 kPa and an intended matric suction (s) of 10 kPa was produced in the same way as in the water retentivity test. The degree of saturation for the unsaturated C-40 specimen was set up in consideration of the degree of saturation for the subbase course of the actual pavement structure during regular seasons, as will be described in a later section.

Upon attaining an equilibrium condition in the consolidation process, the specimens were continuously sheared by applying an axial deviator stress (q) at a designated constant axial strain rate of 0.05%/min under a fully drained condition (CD test) regardless of the water content, while all the other testing parameters were held constant. Note that for the unsaturated testing condition, both pore air and pore water are allowed to drain. The measurement of the air entry value (AEV) for the versapor membrane filter showed that the AEVs, before and after the triaxial compression tests, were nearly equal regardless of the loading methods; this indicates that the versapor membrane filter suffers little degradation of its functions from the wear and tear due to the direct contact with coarse particles. In addition, to evaluate the performance of the new medium-size triaxial apparatus by a comparison with previous research, triaxial compression tests with Toyoura sand were conducted under experimental conditions similar to those in past research (Ishikawa et al., 2010).

3.3.2. Cyclic loading tests

A resilient modulus test (MR test) using the triaxial compression test with cyclic loading on a soil specimen such as "AASHTO Designation: T307-99" and "E016", established with reference to the AASHTO T307-99, is designed to evaluate the resilient deformation characteristics of unbound granular materials, like base course materials/subgrade soils, by simulating the traffic wheel loading on in situ soils. In this

study, the loading conditions standardized by AASHTO for base/subbase materials were employed, as shown in Table 3 and Fig. 5. Here, the axial deviator stress is composed of the cyclic load and the contact load. A haversine-shaped load pulse, with a load duration of 0.1 s followed by a rest period of 0.9 s, that is, a loading frequency of 10 Hz, was applied as the traffic wheel loading on the subbase course material. In addition, as presented in Table 3, the test procedure requires both a conditioning process with 1000 loading cycles (N_c) and an actual testing process with 100 loading cycles under 15 successive paths with varying combinations of confining pressure and deviator stress (Fig. 5). All the tests were conducted under a constant confining pressure. At each confining pressure and deviator stress, the resilient modulus value was determined by averaging the resilient deformation of the last five cycles. Hence, from a single test on a soil specimen under a specified water content, fifteen resilient moduli at different combinations of confining pressure and deviator stress were determined.

After preparing the soil specimens under saturated, unsaturated, and air-dried conditions, in the same way as for the triaxial compression tests with monotonic loading, explained in the preceding section, MR tests on C-40 were performed under a fully drained condition (CD test) as follows. For air-dried and saturated specimens, conventional MR tests were conducted in accordance with AASHTO T307-99. Here, in an air-dried condition, the designated effective confining pressure (σ'_c), shown in Table 3, was applied by providing a specified positive cell pressure (σ_c), keeping the same pore air pressure (u_a) and atmospheric pressure and closing the pore water pressure path. In a saturated condition, it was applied by providing a specified σ_c, maintaining a pore water pressure (u_w) of 200 kPa, and closing the pore air pressure path. For the unsaturated specimen, suction-controlled MR tests were carried out under the prescribed net normal stress (σ_{net}) shown in Table 3 by applying a certain σ_c, while maintaining constant values for u_a and u_w of 200 kPa and 190 kPa, respectively, and keeping both pore pressure paths open.

Table 3
Loading conditions of MR tests.

Name	σ'_c (kPa)	q_{cont} (kPa)	q_{cyclic} (kPa)	q_{max} (kPa)	N_c (cycle)
Conditioning process	103.4	10.3	93.1	103.4	1000
Testing process MR-1	20.7	2.1	18.6	20.7	100
Testing process MR-2	20.7	4.1	37.3	41.4	100
Testing process MR-3	20.7	6.2	55.9	62.1	100
Testing process MR-4	34.5	3.5	31.0	34.5	100
Testing process MR-5	34.5	6.9	62.0	68.9	100
Testing process MR-6	34.5	10.3	93.1	103.4	100
Testing process MR-7	68.9	6.9	62.0	68.9	100
Testing process MR-8	68.9	13.8	124.1	137.9	100
Testing process MR-9	68.9	20.7	186.1	206.8	100
Testing process MR-10	103.4	6.9	62.0	68.9	100
Testing process MR-11	103.4	10.3	93.1	103.4	100
Testing process MR-12	103.4	20.7	186.1	206.8	100
Testing process MR-13	137.9	10.3	93.1	103.4	100
Testing process MR-14	137.9	13.8	124.1	137.9	100
Testing process MR-15	137.9	27.6	248.2	275.8	100

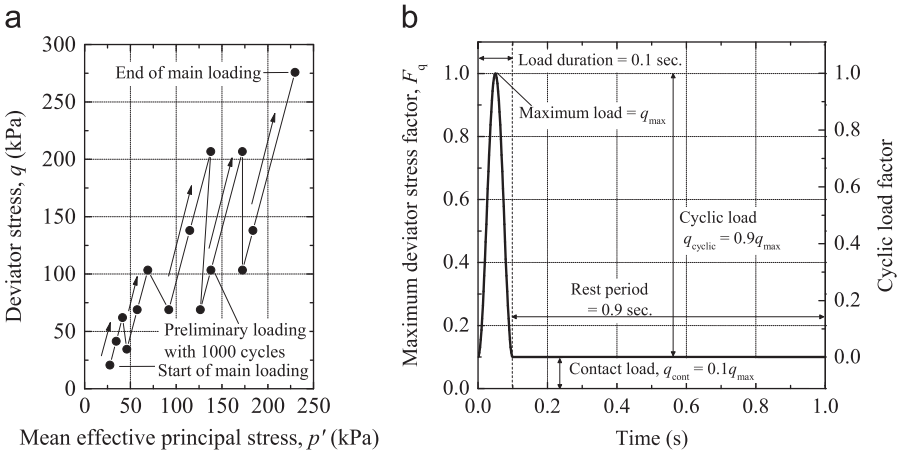

Fig. 5. Loading conditions of MR tests ((a) applied stress path, (b) loading wave).

4. Results and discussions

4.1. Soil–water characteristics

4.1.1. Toyoura sand

Fig. 6 shows the soil–water characteristic curve for Toyoura sand (the relationship between matric suction (s) and volumetric water content (θ)) obtained from water retentivity tests, in comparison to the SWCCs of two former researches. The value of suction (s) in this study is defined by a suction value applied to the specimen through the cap and the pedestal. Note that Abe (1994) performed water retentivity tests on a cylindrical specimen ($H=50$ mm, $D=20$ mm, and void ratio (e) $=0.77$) using the pressure plate method with ceramic disks, while Tokoro et al. (2009) carried out the tests on a cylindrical specimen ($H=70$ mm, $D=30$ mm, and $e=0.66$) using the pressure membrane method with cellulose membrane filters. The SWCC of this study is S-shaped with an inflection point where the matric suction increased as the volumetric water content decreased, and the shape qualitatively matches the results of previous studies. Moreover, the SWCC of this study showed an AEV of 1.48 kPa, determined with reference to Kohgo et al. (1993), and a residual volumetric water content (θ_r) of 4.61%. This AEV is slightly lower than that in the test results by Tokoro et al. (2009) (AEV = 2.30 kPa), and the θ_r in this study is a little higher than that of Abe ($\theta_r=3.4\%$). Although there are minor quantitative differences in the AEV and the θ_r between this study and Abe's (1994) and Tokoro et al.'s (2009), the results of this study are qualitatively in fair agreement with the two past achievements. These results indicate that this test apparatus is highly applicable for water retentivity tests with Toyoura sand. In addition, to insure the reliability of the uniform distribution of the water content inside a large unsaturated specimen, the water content (w) for every layer of 5 cm in height was examined after the water retentivity tests. For example, the results show $w=4.06\%$, 4.22%, and 5.22% for layers of 0–5 cm, 5–10 cm, and 10–15 cm away from the end of the specimen, respectively. This indicates that the distribution of water content against the height could be almost uniform in the range within 10 cm from both ends where the matric suction is well controlled, although the water content tends to increase a little toward the center of the specimen from the edge.

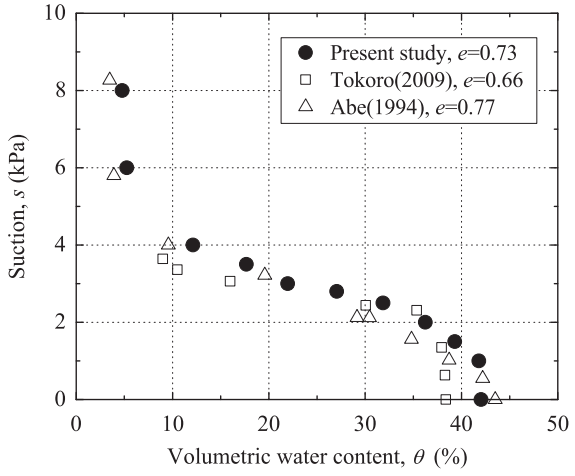

Fig. 6. Soil–water characteristic curves of Toyoura sand.

The total testing time for a water retentivity test mainly depends on the time it takes to achieve an equilibrium between the matric suction and the water content when increasing the matric suction, namely, the elapsed time until the drainage from the specimen stops. Regarding the reduction of testing time, Ishikawa et al. (2010) reported that the drainage time, brought about by the application of matric suction to the specimen, was reduced to 1/100 in a test that adopted the pressure membrane method instead of the pressure plate method. Thus, we compared the testing time reported by Tokoro et al. (2009) with that obtained from this study, both of which used the same pressure membrane method. Although there was no clear difference in the area ratio of the water supply/drain paths against the cross section of the specimen, the equilibrium time required in the case of increasing the matric suction from $s=0$ to 2.0 kPa was 1368 min for this study and 84 min for Tokoro et al. (2009). Thus, the testing time in this study was 16.3 times longer than that of Tokoro et al. (2009). However, the height of the specimen in this study was 10 times that of Tokoro et al. (2009). Considering that the coefficient of permeability or the thickness of a versapor membrane filter is nearly equal to that of a cellulose membrane filter, and that the equilibrium time is generally proportional to the square of the specimen height, the drainage rate in this study is fairly fast for the large specimen size. One possible reason is that this study employed double drainage from both end faces, which made the maximum drainage length half of the specimen height. In contrast, Tokoro et al. (2009) conducted a water retentivity test with single drainage from the top surface of the specimen. In fact, the equilibrium time required for the increment in matric suction from $s=0$ to 2.0 kPa, when the water retentivity test was conducted with single drainage using the new medium-size triaxial apparatus, was 5206 min, which is 3.81 times longer than with the double drainage under the same experimental conditions. These results indicate that double drainage using the pressure membrane method is effective for reducing the total testing time in water retentivity tests with large specimens, as was the case in this study.

4.1.2. Subbase course material (C-40)

To evaluate the applicability of the medium-size triaxial apparatus to water retentivity tests for coarse granular materials, Fig. 7 shows the SWCCs for C-40 with the D_c of 95% and 90% obtained from this study. The SWCC obtained from the water retentivity test on a cylindrical specimen ($H=125$ mm, $D=150$ mm, and $D_c=95\%$), using the suction method (Yano et al., 2011), and the SWCC obtained from the test on a cylindrical specimen ($H=480$ mm, $D=305$ mm, and $D_c=98\%$), using the soil column method (Ishigaki and Nemoto, 2005) are also shown. Unlike the SWCC for Toyoura sand, the SWCC for C-40 was a J-shaped curve with no clear boundary effect area or AEV, owing to the rapid drainage concurrent with the application of matric suction. The shape of

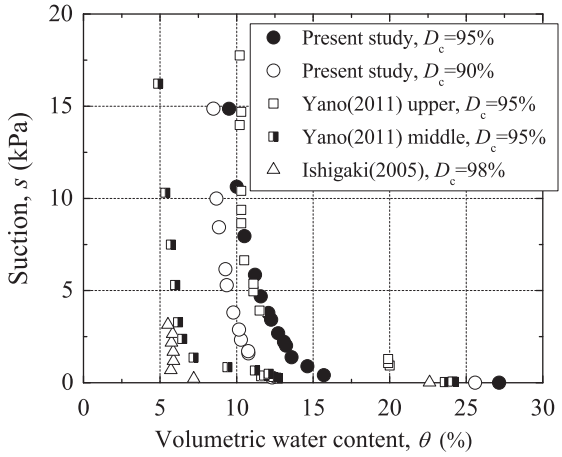

Fig. 7. Soil–water characteristic curves of C-40.

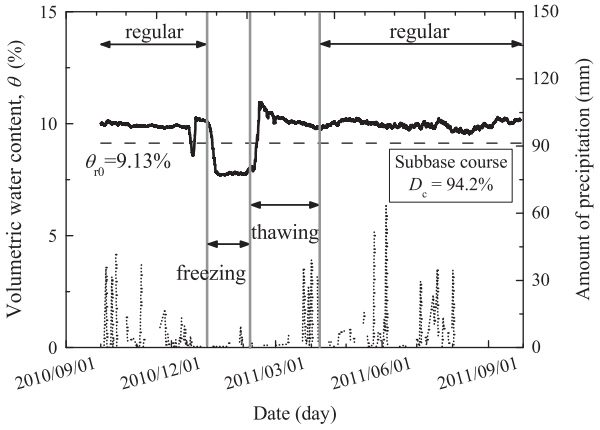

Fig. 8. Results of long-term field measurements.

the SWCC hardly changes in accordance with D_c, although the location of the SWCC moves toward the left so as to decrease the water retentivity when D_c decreases even for the same sample. In addition, the θ_r value for C-40 (D_c=95%) was 9.13%, which indicates that the water retentivity is higher than that of Toyoura sand. This is considered ascribable to the fact that C-40 is well-graded and has a higher fines content than Toyoura sand. Note that based on the measurement of the water absorption into crushed stone particles during water retentivity tests pursuant to "Methods of test for density and water absorption of coarse aggregates" (JIS A 1110), there was no water absorption or drainage to or from the soil particles after the consolidation, indicating that the volumetric water content in this study does not depend on the water absorption of the soil particles.

Next, we compared the SWCC for C-40 obtained from this study with the results of previous studies. Based on Table 2, the C-40 sample used in this study shows physical properties relatively similar to those of C-40 used in other researches, and the grain-size distribution was intermediate between coarse C-40, like "Yano (2011) upper", fine C-40, like "Yano (2011) middle", and "Ishigaki (2005)", as shown in Fig. 4. Although the SWCC of this study differs a little in the shape at the boundary effect zone (Vanapalli et al., 1996) from the SWCC of "Yano (2011) upper", SWCCs indicating that the AEV of C-40 is extremely small, like this study, can be seen in "Ishigaki (2005)" and "Yano (2011) middle". Meanwhile, the θ_r of 9.13% in this study is higher than the results of "Yano (2011) middle" and "Ishigaki (2005)" by approximately 5%, and a little lower than the results of "Yano (2011) upper". These differences are mainly attributed to the differences in grain-size distribution, fines content, and the degree of compaction of the test specimens between this study and past researches. Accordingly, it can be concluded that the medium-size triaxial apparatus for unsaturated soils has a high applicability to water retentivity tests on coarse granular materials.

Finally, we compared the above-mentioned results with the results of the long-term field measurements of an actual pavement structure in Hokkaido. Fig. 8 shows the daily change in water content measured at the subbase course of the test pavement along with the daily amount of precipitation. The subbase course of the test pavement was composed of the same C-40 used in this study, although the degree of compaction was slightly lower than D_c=95%. From Fig. 8, it is evident that the volumetric water content (θ) during the normal seasons, except for the freezing season and the thawing season, was nearly stable at around 10%, and that it temporarily increased from the level before freezing to the peak of approximately 11% during the thawing season. Compared to Fig. 7, the θ at the actual subbase course during the normal seasons nearly conformed to the residual degree of saturation (θ_r), and it was considerably lower than the θ of 16% that corresponded to the optimal water content. It is thought, therefore, that the water content of the subbase course during the normal seasons is close to the residual volumetric water content in the actual pavement structure. It is also assumed that the changes in water content, observed from the normal seasons to the thawing season, seriously influence the mechanical behavior of granular base course materials. This is because it corresponds to the transitional area from the pendular saturation to the fuzzy saturation, where matric suction dramatically fluctuates against changes in the volumetric water content.

4.2. Deformation–strength characteristics under monotonic loading

4.2.1. Stress–strain relationship for Toyoura sand

Fig. 9 shows a typical relationship between the axial deviator stress (q), the volumetric strain (ε_v), and the axial strain (ε_a) obtained from the monotonic loading CD test on Toyoura sand under an unsaturated condition (s=2.5 kPa and S_r=82.3%), in comparison to the stress–strain-dilatancy relationship derived from Ishikawa et al. (2010) with a cylindrical specimen (H=170 mm, D=70 mm, and e=0.66). Note that for the test on Toyoura sand, the axial strain was calculated based on the axial displacement measured by an external displacement transducer (Fig. 3) to ensure consistency with the measuring method of the axial strain in the previous study. Although the specimen may not reach the residual state, owing to an accident in this study, the

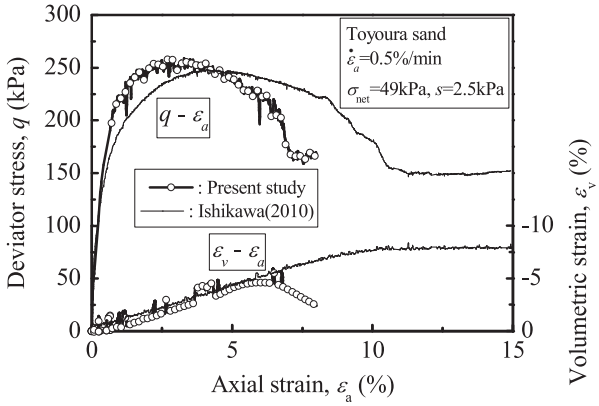

Fig. 9. Stress–strain relationships of Toyoura sand.

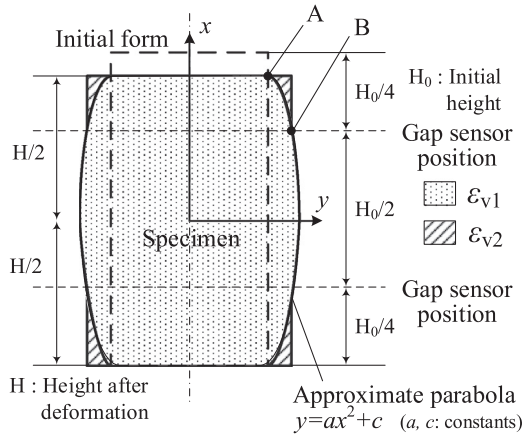

Fig. 10. Calculation methods for volumetric strain.

strain-softening behavior in which the deviator stress decreased with increments in axial strain after the deviator stress reached the maximum value at an axial strain of 5% or lower, was observed in both stress–strain relationships. Moreover, although the soil specimen initially dilates with the increment in ε_a during shear, it reaches a constant volume condition at a large ε_a of 10% or more. These tendencies toward stress–strain-dilatancy relationships can be observed regardless of the testing method, and almost no quantitative difference in peak strength or volumetric strain up to the maximum deviator stress between the two testing methods can be detected. It is thus surmised that this test apparatus is highly applicable to triaxial compression tests on geomaterials like sand.

4.2.2. Evaluation of measurement precision at tests for C-40

The reliability of the measurement system in triaxial compression tests with a medium-size triaxial apparatus for unsaturated coarse granular materials should be checked. Firstly, we discuss the applicability of the calculation method for volumetric strain using gap sensors. This study employs the average value (ε_v(GS)) of volumetric strain (ε_{v1}) and (ε_{v2}), derived from two different calculation methods, as the volumetric strain, as shown in Fig. 10. Here, ε_{v1} was calculated supposing that the specimen after shear has a vertical cross section, like the shape of a beer barrel, whose curved boundary is approximated by a parabola with reference to Kato and Kawai (2000), while ε_{v2} was calculated supposing that the specimen diameter uniformly spreads like a cylinder regardless of the height. In calculating ε_{v1}, by separately determining the parabola functions for the upper and lower parts of the specimen from the lateral displacement and height at the position of the gap sensors (e.g., point B in Fig. 10) and the end of the specimen (e.g., point A in Fig. 10), we assume that neither end of the specimen spreads in the radial direction, and that the volume of the specimen is equivalent to that of the two rotators of the parabola around the x-axis. Note that with the assumption that the axial strain caused by shear is constant over the whole specimen, the positions of the gap sensors are compensated in accordance with the measured axial strain (ε_a).

Fig. 11 shows the relationships between volumetric strain (ε_v) and axial strain (ε_a) obtained from triaxial compression

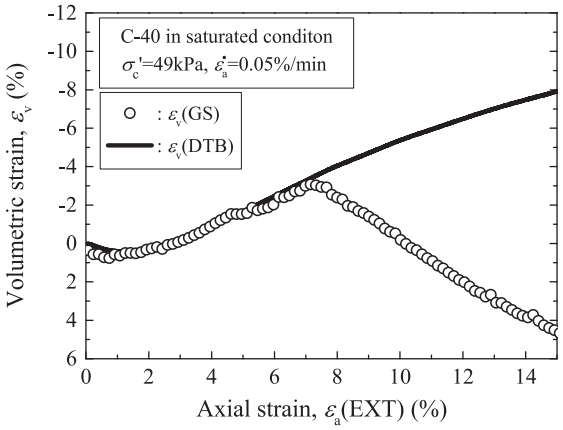

Fig. 11. Comparison of ε_v obtained from different measuring methods.

tests with monotonic loading on saturated C-40. Here, ε_v(GS) and ε_v(DTB) are the volumetric strains measured by the gap sensors and the double tube buret system, respectively, while ε_a(EXT) is the axial strain measured by an external displacement transducer (EXT). Measurements by the two methods are in reasonable agreement with each other in terms of the change in volumetric strain during shear up to the axial strain of 7%, that is, until the deviator stress reaches the peak, as will be seen in the stress–strain relationship of saturated C-40 (Fig. 14). However, the ε_v(GS)–ε_a(EXT) relation after the axial strain of 7% or larger is markedly different from the ε_v(DTB)$-\varepsilon_a$(EXT) relation. A tendency, similar to that in Fig. 11, was observed irrespective of the calculation method for volumetric strain. For reference, according to three preliminary tests for saturated C-40 under various levels of effective confining pressure, the average coefficients of determination between ε_v(DTB) and various volumetric strains (ε_{v1}, ε_{v2}, and ε_v(GS)), calculated based on the different approximations mentioned above in the range of an axial strain up to around 7%, were 0.94 for ε_{v1}, 0.96 for ε_{v2}, and 0.98 for ε_v(GS), respectively. This confirms the validity of the calculation method for the volumetric strain employed in this study. Accordingly, the reason for the difference between ε_v(GS) and ε_v(DTB), seen in Fig. 11, is that the proposed

method which calculates the overall deformation of the specimen from the lateral displacements, measured at the installed locations of the gap sensors, cannot sufficiently estimate the strain-softening deformation behavior where the localization of deformation into shear band dramatically develops with the sharp decrease in the shear resistance of the soil when the applied load exceeds the peak strength, especially for large triaxial specimens. A similar phenomenon is also observed in the triaxial compression tests on Toyoura sand (Fig. 9), showing the same strain-softening behavior. There is a room for further investigation as to the validity of the measuring method of the volumetric strain for post-peak behavior. However, the objective of this research is to propose a laboratory element test for evaluating the mechanical response of unsaturated subbase course in asphalt pavement under traffic loads, and therefore, the stress level that should be dealt with in this paper corresponds to the pre-failure behavior of base course materials. This means that it is not necessary to enter into a detailed discussion on the behavior after the peak strength for the purpose of this study. Consequently, we do not adopt ε_v(GS) here as experimental data in the range of axial strain over the peak strength from the viewpoint of measurement precision.

Next, we discuss the influence of system compliance (SC) and bedding errors (BE) in laboratory element tests on geomaterials, as they have been addressed as problems encountered in accurately measuring the axial displacement with an external displacement transducer, especially in triaxial compression tests for hard geomaterials such as gravel (Tatsuoka and Shibuya, 1992). Fig. 12 shows typical relationships between the deviator stress (q) and various kinds of axial strain (ε_a) obtained from triaxial compression tests with monotonic loading on saturated C-40. Here, ε_a(LVDT) and ε_a(LLVDT) are the axial strain measured by two types of linear variable differential transformers (LVDTs and LLVDTs, respectively). When comparing axial strain measured at different locations in the range up to 2% of ε_a (EXT), the value under the same q increased in order of ε_a(LLVDT), ε_a(LVDT), and ε_a(EXT), regardless of the stress level. In this case, the difference between ε_a(LVDT) and ε_a(EXT) mainly indicates the effect of SC, while the difference between ε_a(LLVDT) and ε_a(LVDT) mainly explains the effect of BE.

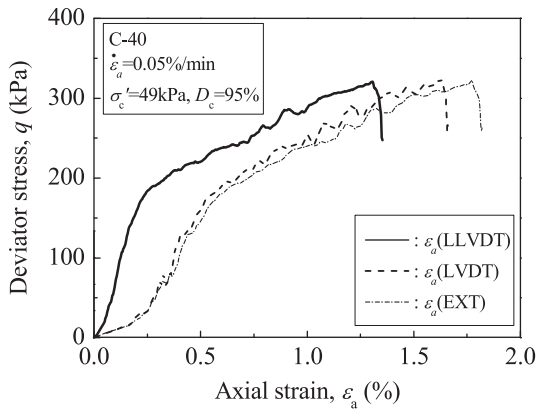

Fig. 12. Comparison of ε_a obtained from different measuring methods.

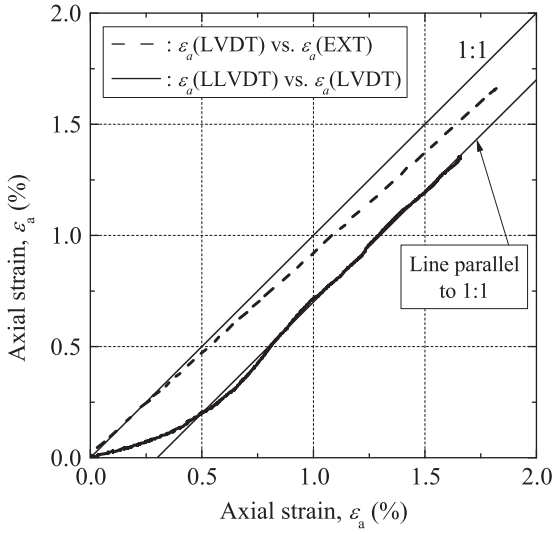

Fig. 13. Measuring error due to SC and BE.

Fig. 13 shows the ε_a(EXT)–ε_a(LVDT) relation and the ε_a(LLVDT)−ε_a(LVDT) relation. The measuring error caused by SC is approximately 10% of ε_a (EXT) in this study because ε_a(LVDT) is almost 90% of ε_a(EXT), and the effect is nearly stable regardless of the strain level. Meanwhile, the effect of BE tends to appear more strongly during the initial loading stage, since the increasing rate of ε_a(LLVDT) due to loading q is small in comparison to that of ε_a(LVDT) in the range lower than about ε_a(LVDT)=0.5%, although the increasing rate of ε_a(LLVDT) is almost equal to that of ε_a(LVDT) over ε_a(LVDT)=0.5%. Accordingly, the effects of SC and BE need to be evaluated when examining the deformation behavior of C-40. This study hereafter employs the corrected value of the axial strain (ε_a) measured by the EXT and the LVDT in consideration of the above-mentioned measuring errors.

4.2.3. Stress–strain relationship for subbase course material (C-40)

Fig. 14 shows typical stress–strain-dilatancy relationships obtained from the monotonic loading CD tests on C-40 under air-dried, unsaturated, and saturated conditions. The dense compacted C-40 exhibits strain-softening behavior in which an increasing axial strain causes a sharp increase in the deviator stress (q) to the peak strength at an axial strain of about 4–6%, and then it gradually decreases to the residual strength at ε_a=12% or over, irrespective of the water content of the specimen. In this case, the maximum deviator stress increased in the order of saturated, unsaturated, and air-dried specimens; the axial strain under the same deviator stress was largest for the air-dried specimen, followed by unsaturated and saturated specimens when we compared them in the range up to a principal stress ratio (σ'_1/σ'_3) of approximately 13, namely q=588 kPa. This phenomenon is thought to have been caused by the decrease in frictional resistance between soil particles due to an increase in the water content along with a decrease in the apparent cohesion owing to the reduction in matric suction. Meanwhile, the specimen dilates with the increment of ε_a during shear after the volume of specimens initially decreases,

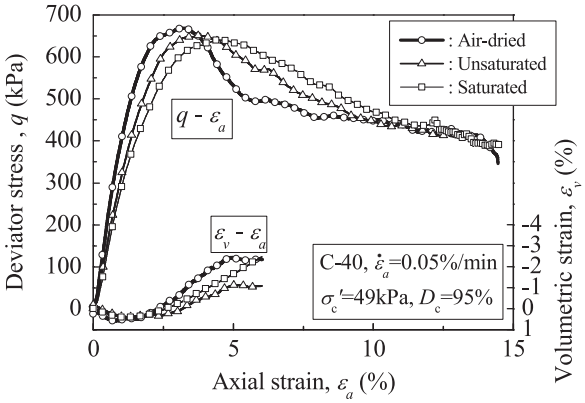

Fig. 14. Stress–strain relationships of C-40.

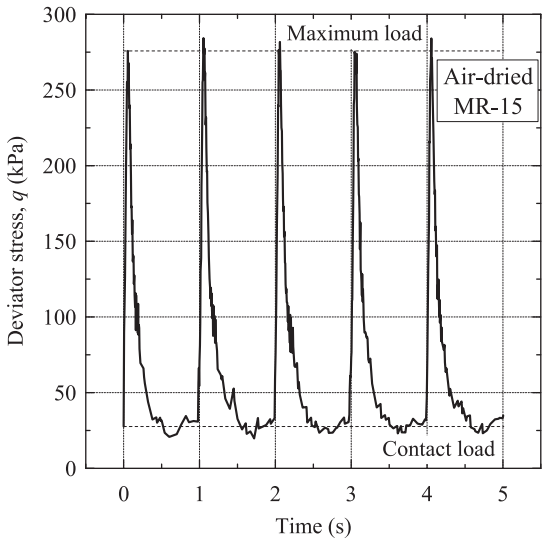

Fig. 15. Example of cyclic loading waves measured in MR tests.

regardless of the water content. In this case, the positive dilatancy tends to be stronger in the order of unsaturated, saturated, and air-dried specimens. This phenomenon is also thought to be caused by the high capillary force in the menisci between grains which attempts to maintain the soil skeleton structure of the unsaturated soils, as Karube and Kato (1994) pointed out. These results indicate that the water content of the specimen has a considerable influence on the deformation–strength characteristics of C-40 in the triaxial compression tests.

4.3. Cyclic deformation characteristics of unsaturated C-40

To evaluate the resilient deformation characteristics of unbound granular subbase course materials, the performance of the medium-size triaxial apparatus was discussed by performing MR tests on C-40 under different water contents. Fig. 15 shows an example of loading waves measured at the MR-15 shown in Table 3. It is recognized that the intended haversine-shaped load pulses were almost reproduced using the hybrid actuator. Moreover, Fig. 16 shows typical relationships at the last five cycles in MR-15 between deviator stress q and axial strain ε_a obtained from the MR tests on C-40 under air-dried, unsaturated, and saturated conditions. Irrespective of the water content, the loading and unloading of deviator stress evidently cause the formation of small clear hysteresis-loops with elasticity showing little residual axial strain, and the deformation behavior of subbase course materials after preliminary cyclic loading seems to exhibit almost constant stiffness at each water content, thus demonstrating the reliability of the testing methodology in this study. In addition, a virgin loading curve generally exhibits a stress–strain relationship with a convex loading curve, while a loading curve after preliminary cyclic loading (Fig. 16) shows a slightly concave shape, which illustrates the non-linearity of the deformation behavior, i.e., the increase in stiffness with q. The difference between them is caused by the fact that the plastic deformation in the stress–strain relationship is dominant in the early stages of cyclic loading, whereas the deformation behavior becomes elastic with the increment in loading cycles. In addition, due to the decrement of the water content, the deformation behavior of the test specimen became stiffer and more elastic. These results indicate that the water content of the specimen and the applied stress level have a considerable influence on the resilient deformation characteristics of C-40 in the MR tests.

Next, we discuss the influence of the water content and the stress state on the resilient deformation characteristics of unbound granular subbase course materials in terms of the resilient modulus (M_r). Fig. 17 shows the relationships between the M_r and the mean principal net stress (p_{net}) or the deviator stress (q), respectively, obtained from suction-controlled MR tests on C-40 in an unsaturated condition. Here, M_r is defined as q_{cyclic}/ε_r (ε_r: resilient or recovered axial strain due to q_{cyclic} in Fig. 5(b)). For plots with the same net normal stress (σ_{net}), the M_r decreases with the increase in the p_{net} and q, while for plots with the same p_{net} and q, the M_r increases with an increase in the σ_{net}. A dominant effect for the deformation behavior of C-40 is an increase in M_r with increasing confining pressure. A similar tendency was observed in the MR tests under saturated and air-dried conditions. Accordingly, as in past researches like the AASHTO standards pointed out, the M_r of the subbase course

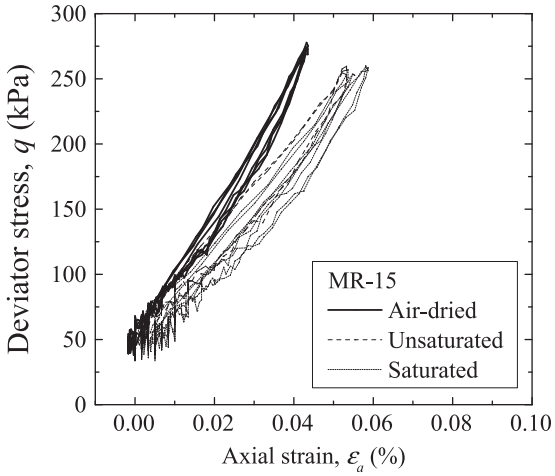

Fig. 16. Comparison of hysteresis-loops in MR tests under different water contents.

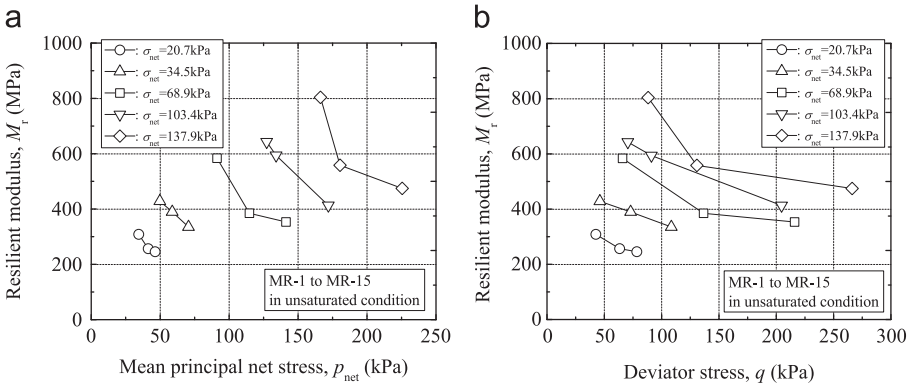

Fig. 17. Influence of stress condition on M_r in unsaturated condition ((a) effect of p_{net}, (b) effect of q).

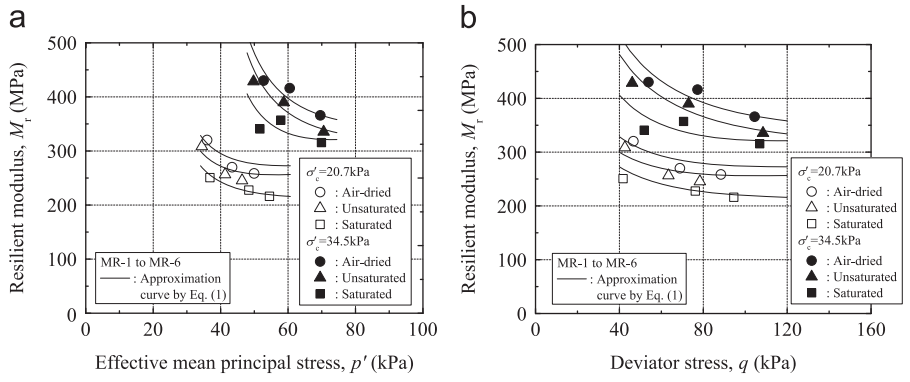

Fig. 18. Influence of stress condition on M_r under various water contents ((a) effect of p', (b) effect of q).

materials measured in this study exhibits strong stress-dependency. The MEPDG (AASHTO, 2008) utilizes a resilient modulus constitutive equation provided in Eq. (1) (Yan and Quintus, 2002). The model is generally referred to as a "universal model" with the advantage of being able to consider the stress state (i.e., normal and shear stress) of the material during the MR tests:

$$M_r = k_1 p_a \left(\frac{\sigma_{ii}}{p_a}\right)^{k_2} \left(\frac{\tau_{oct}}{p_a} + 1\right)^{k_3} \quad (1)$$

where k_1, k_2, and k_3 are regression constants, σ_{ii} is the bulk stress ($\sigma_{ii} = \sigma_1 + \sigma_2 + \sigma_3$), p_a is the normalizing stress, and τ_{oct} is the octahedral shear stress. It should be noted that the octahedral shear stress becomes $(\sigma_1 - \sigma_3)$ for the axisymmetric stress condition. Fig. 18 examines the applicability of Eq. (1) to test results under the effective confining pressure levels (σ'_c) of 20.7 kPa and 34.5 kPa. When comparing the plots with the same p_{net} or q under the same σ'_c, the remarkable decreasing tendency of M_r followed by the increase in the water content is recognized irrespective of σ'_c. The stress-dependency of M_r derived from this study agrees well with the regression analysis results of Eq. (1), regardless of the water content. Accordingly, it seems reasonable to conclude that the suction-controlled MR test results for C-40 in this study qualitatively match those of previous studies.

On the other hand, the degradation in the CBR (California Bearing Ratio), associated with the increase in water content in the CBR tests on the same C-40, was reported by Kawabata et al. (2012). Fig. 19 compares the M_r estimated by the following empirical formulas adopted in the AASHTO standards with the M_r derived from the approximation curves shown in Fig. 18. The latter is the one at the principal stress ratio (σ'_1/σ'_3) of 4 under the σ'_c of 20.7 kPa, that is, the stress state closely analogous to the stress states of an actual Japanese pavement structure calculated using a multi-layered elastic analysis (Ishikawa et al., 2012). The secant deformation moduli (E_{sec}) at the σ'_1/σ'_3 of 4 under different water contents calculated from the stress–strain relationships (Fig. 14) in monotonic loading CD tests were also plotted. Here, the E_{sec} was calculated from $(\sigma'_1 - \sigma'_3)/\varepsilon_a$ (AASHTO, 1993, 2008):

$$M_r(\text{MPa}) = 3.03 \times CBR \quad (2)$$

$$M_r(\text{MPa}) = 17.6 \times CBR^{0.64} \quad (3)$$

Under the same water content, the E_{sec} is noticeably lower than the M_r derived from the MR tests because it includes the plastic deformation of the material. However, the decreasing tendencies of all types of M_r and E_{sec}, with an increasing water content, are in fair agreement with each other, irrespective of the calculation method. Based on the above-mentioned results, it can be concluded that the medium-size triaxial apparatus for unsaturated soils has high applicability in the evaluation of the resilient deformation characteristics of unbound granular subbase course materials.

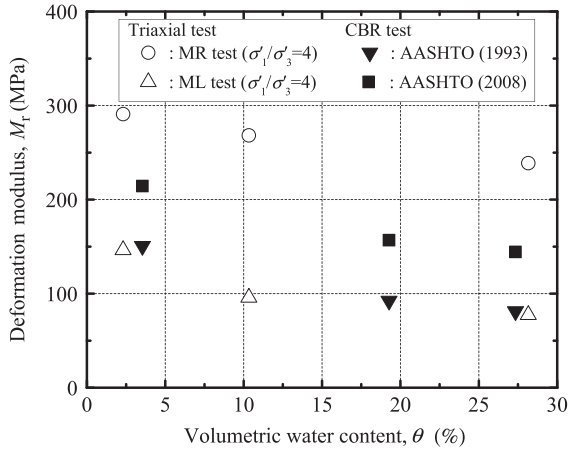

Fig. 19. Influence of water content on M_r estimated by different calculation methods.

5. Conclusions

The following findings have been obtained from the present study:

(1) This study newly developed a medium-size triaxial apparatus for unsaturated soils, as a laboratory element test of high practical use, suitable for evaluating the mechanical behavior of unsaturated coarse granular materials. The apparatus can perform both monotonic loading tests and cyclic loading tests on C-40 under various water contents by using strain-controlled and stress-controlled methods with high precision and variable loading rates.

(2) The apparatus adopts the pressure membrane method, instead of the pressure plate method, and installs water supply/drainage paths on both the cap and the pedestal to reduce the total testing time. As a result, the double drainage through the hydrophilic microporous membrane filters proposed in this study can considerably reduce the testing time in water retentivity tests and triaxial compression tests with a medium-size specimen under an unsaturated condition as compared to conventional testing methods.

(3) The water retention characteristics and deformation–strength characteristics of the unsaturated sands and crusher-run obtained from this study agree well with the previously published experimental data. They demonstrate that the water content has a considerable influence on the deformation–strength characteristics of unbound granular subbase course materials, namely, the peak shear strength and the deformation modulus decrease with an increasing water content.

This study has proposed a suction-controlled laboratory element test with the newly developed medium-size triaxial apparatus for unsaturated soils in order to quantitatively evaluate the effects of the water content on the mechanical behavior of unbound granular subbase course materials. The foregoing findings confirm the high applicability and the excellent usefulness of the developed test apparatus and the proposed testing method to water retention tests and suction-controlled triaxial compression tests on unsaturated subbase course materials in terms of the validity of the test results and the reduction of total testing time. However, as the findings of this study were obtained under limited experimental conditions, continuing an examination of their validity and applicability will be necessary as a future work before practical application.

Acknowledgments

The authors would like to thank Mr. Hirosato Segawa (formerly of Hokkaido University), who performed the laboratory shear tests and arranged the experimental results. This research was supported in part by Grant-in-Aid for Scientific Research (B) (20360206) from the Japan Society for the Promotion of Science (JSPS) KAKENHI.

References

AASHTO. 1986. Standard method of test for resilient modulus of subgrade soils, AASTHO Designation T 274-82. In: Standard Specifications for Transportation Materials and Methods of Sampling and Testing, pp. 1198–1218.

AASHTO. 1993. AASHTO Guide for Design of Pavement Structures, Washington.

AASTHO. 2003. Standard method of test for determining the resilient modulus of soils and aggregate materials, AASTHO Designation T 307-99. In: Standard Specifications for Transportation Materials and Methods of Sampling and Testing, T307-1-T-307-41.

AASHTO. 2008. Mechanistic-Empirical Pavement Design Guide: A Manual of Practice, Washington.

Abe, H. 1994. Experimental study on the estimation of mechanical properties for unsaturated soils (Ph.D. Thesis), University of Tokyo, Tokyo (in Japanese).

Burland, J.B., 1989. Ninth Laurits Bjerrum Memorial Lecture: Small is beautiful – the stiffness of soils at small strain. Can. Geotech. J. 26 (4), 499–516.

Cary, C.E., Zapata, C.E., 2010. Enhanced model for resilient response of soils resulting from seasonal changes as implemented in mechanistic-empirical pavement design guide. Transp. Res. Record: J. Transp. Res. Board 2170, 36–44.

Coronado, O., Fleureau, J., Correia, A., Caicedo, B. 2005. Influence of suction on the properties of two granular road materials. In: I. Horvli (Ed.), Proceedings of the 7th International Conference on the Bearing Capacity of Roads, Railways and Air-fields, Trondheim, 27–29 June 2005 [1/1(CD-ROM) 260].

Craciun, O., Lo, S.-C.R., 2012. Matric suction measurement in stress path cyclic triaxial testing of unbound granular base materials. Geotechn. Test. J. 33 (1), 33–44.

Dawson, A.R., Gillett, S.D., 1998. Assessment of on-sample instrumentation for repeated load triaxial tests. Transp. Res. Record: J. Transp. Res. Board 1614, 52–60.

Ekblad, J., Isacsson, U. 2008. Water in coarse granular materials: Resilient and retentive properties. In: Ellis, Yu, McDowell, Dawson, Thom (Eds.), Proceedings of the International Conference on Advances in Transportation Geotechnics, Nottigham, 25–27 August 2008, pp. 117–123.

Fredlund, D.G., 2006. Unsaturated soil mechanics in engineering practice. J. Geotech. Geoenviron. Eng. 132 (3), 286–321.

Ishigaki. T., Nemoto, S. 2005. A study on water retention and permeability characteristics of granular base course materials. In: Proceedings of the 60th Annual Conference of the Japan Society of Civil Engineers, vol. 5, pp. 117–118 (in Japanese).

Ishikawa, T., Kawabata, S., Kameyama, S., Abe, R., Ono, T. 2012. Effects of freeze–thawing on mechanical behavior of granular base in cold regions. In: Miura, Ishikawa, Yoshida, Hisari, Abe (Eds.), Proceedings of the International Conference on Advances in Transportation Geotechnics II, Sapporo, 10–12 September 2012, pp. 118–124.

Ishikawa, T., Tokoro, T., Ito, K., Miura, S., 2010. Testing methods for hydro-mechanical characteristics of unsaturated soils subjected to one-dimensional freeze–thaw action. Soils Found. 50 (3), 431–440.

Japanese Geotechnical Society. 2000a. Method for consolidated drained triaxial compression test on soils (JGS 0524-2000). Standards of Japanese Geotechnical Society for Laboratory Shear Test, pp. 23–27.

Japanese Geotechnical Society. 2000b. Method for triaxial compression test on unsaturated soils (JGS 0527-2000). Standards of Japanese Geotechnical Society for Laboratory Shear Test, pp. 40–46.

Japanese Geotechnical Society. 2009. Test method for water retentivity of soils (JGS 0151-2009). Standards of Japanese Geotechnical Society for Laboratory Soil Testing Methods, pp. 162–169 (in Japanese).

Japan Road Association (Eds.). 2006. Pavement Design Manual, Tokyo. (in Japanese).

Japan Road Association (Eds.). 2007. Handbook of pavement investigation and examination methods, Tokyo. (in Japanese).

Karube, D., Kato, S. 1994. An ideal unsaturated soil and the Bishop′s soil. In: Proceedings of the 13th International Conference on Soil Mechanics and Foundation Engineering, New Delhi, India, 5–10 January, Taylor & Francis, New York, vol. 1, pp. 43–46.

Kato, S., Kawai, K., 2000. Deformation characteristics of a compacted clay in collapse under isotropic and triaxial stress state. Soils Found. 40 (5), 75–90.

Kawabata, S., Ishikawa, T., Murayama, T., Kameyama, S., 2012. Effect of freeze–thawing on bearing capacity of granular base course material. J. Jpn. Soc. Civil Eng. Div. E 68 (3), I_115–I_122 (in Japanese).

Kohgo, Y., Nakano, M., Miyazaki, T., 1993. Theoretical aspects of constitutive modelling for unsaturated soils. Soils Found. 33 (4), 49–63.

Kolisoja, P., Saarenketo, T., Peltoniemi, H., Vuorimies, N., 2002. Laboratory testing of suction and deformation properties of base course aggregates. Transp. Res. Record 1787, 83–89.

Miura, S., Toki, S., 1982. A sample preparation method and its effect on static and cyclic deformation–strength properties of sand. Soils Found. 22 (1), 61–77.

Nazarian, S., Pezo, R.F., Melarkode, S., Picornell, M., 1997. Testing methodology for resilient modulus of base materials. Transp. Res. Record 1547, 46–52.

Nishimura, T., Koseki, J., Fredlund, D.G., Rahardjo, H., 2012. Microporous membrane technology for measurement of soil-water characteristic curve. Geotechn. Test. J. 35 (1), 1–8.

Tatsuoka, F., Lo Presti, D.C.F., Kohata, Y. 1995. Deformation characteristics of soils and soft rocks under monotonic and cyclic loads and their relations. In: 3rd International Conference on Recent Advances in Geotechnical Earthquake Engineering and Soil Dynamics: State of the Art 1,2, pp. 851–879.

Tatsuoka, F., Shibuya, S. 1992. Deformation characteristics of soils and rocks from field and laboratory tests. In: D. Toll (Ed.), Proceedings of the International 9th Asian Regional Conference on Soil Mechanics and Geotechnical Engineering, 9–13 December 1991, vol. 2, pp. 101–170.

Tokoro, T., Ishikawa, T., Miura, S. 2009. Effect of the cross section of plumbing path on coefficient of permeability of unsaturated sand. In: Proceedings of the 44th Annual Conference of the Japan Society of Civil Engineers 3: 963–964 (in Japanese).

Tutumluer, E., Garg, N., Thompson, M.R., 1998. Granular material radial deformation measurements with a circumferential extensometer in repeated load triaxial testing. Transp. Res. Record 1614, 61–69.

Vanapalli, S.K., Fredlund, D.G., Pufahl, D.E., Clifton, A.W., 1996. Model for the prediction of shear strength with respect to soil suction. Can. Geotechn. J. 33 (3), 379–392.

Yan, A., Quintus, H.L.V. 2002. Study of LTPP Laboratory Resilient Modulus Test Data and Response Characteristics: Final Report, Publication No. FHWA-RD-02-051, U.S. Department of Transportation, Federal Highway Administration, McLean, VA: 1–161.

Yano, T., Nishiyama, S., Nakashima, S., Moriishi, K., Ohnishi, Y., 2011. Saturated-unsaturated hydraulic properties of subbase course material and subgrade soil. J. Jpn. Soc. Civ. Eng. Div. E1 67 (2), 120–130 (in Japanese).

Zhang, L.M., Li, X., Fredlund, D.G. 2009. SWCCs and permeability functions for coarse-grained soils. In: Buzzi, Fityus, Sheng (Eds.), Proceeding of the International 4th Asia-Pacific Conference on Unsaturated Soils, Newcastle, Australia, 23–25 November 2009, pp. 251–256.